Morphology, histochemistry and glycosylation of the placenta and associated tissues in the European hedgehog (Erinaceus europaeus)

DOI:
10.1016/j.placenta.2016.09.010

*Title Page and Abstract

Morphology, histochemistry and glycosylation of the placenta and associated tissues in the European hedgehog (*Erinaceus europaeus*)

Carolyn J. P. Jones[a*], A. M. Carter[b], W. R. Allen[c] and Sandra A. Wilsher[c]

[a]Maternal and Fetal Health Research Centre, Division of Developmental Biology and Medicine, School of Medical Sciences, Faculty of Biology, Medicine and Health, University of Manchester, St Mary's Hospital, Oxford Road, Manchester M13 9WL, U.K.

[b]Cardiovascular and Renal Research, Institute of Molecular Medicine, University of Southern Denmark, Odense, Denmark.

[c]The Paul Mellon Laboratory, "Brunswick", 18 Woodditton Road, Newmarket, Suffolk CB8 9BJ, U.K.

***Author for correspondence:** Dr Carolyn Jones, Maternal and Fetal Health Research Centre, Division of Developmental Biology and Medicine, School of Medical Sciences, Faculty of Biology, Medicine and Health, University of Manchester, St Mary's Hospital 5th floor (Research), Oxford Road, Manchester M13 9WL

Tel: 44(0)161 701 6953
Fax: 44(0)161 701 6971
Email: carolyn.jones@manchester.ac.uk

Abstract

Introduction. There are few descriptions of the placenta and associated tissues of the European hedgehog (*Erinaceus europaeus*) and here we present findings on a near-term pregnant specimen.

Methods. Tissues were examined grossly and then formalin fixed and wax-embedded for histology and immunocytochemistry (cytokeratin) and resin embedded for lectin histochemistry.

Results: Each of four well-developed and near term hoglets displayed a discoid, haemochorial placenta with typical labyrinth and spongy zones. In addition there was a paraplacenta incorporating Reichert's membrane and a largely detached yolk sac. The trophoblast of the placenta contained diverse populations of granule which expressed most classes of glycan. Intercellular membranes were also glycosylated and this tended to be heavier in the labyrinth zone. Fetal capillary endothelium had glycosylated apical surfaces expressing sialic acid and various other glycans. Glycogen was present in large cells situated between the spongy zone and the endometrium. Trophoblast cells in the placental disc and under Reichert's membrane, as well as yolk sac endoderm and mesothelium, were cytokeratin positive. Reichert's membrane was heavily glycosylated. Yolk sac inner and outer endoderm expressed similar glycans except for N-acetylgalactosamine residues in endodermal acini.

Discussion. New features of near-term hedgehog placenta and associated tissues are presented, including their glycosylation, and novel yolk sac acinar structures are described. The trophoblast of the placental disc showed significant differences from that underlying Reichert's membrane while the glycan composition of the membrane itself showed some similarity to that of rat thereby implying a degree of biochemical conservation of this structure.

Key words: Placenta; Reichert's membrane; yolk sac; histology; lectins; cytokeratin

Highlights

- The near-term placenta of ***Erinaceus europaeus*** was discoid and haemochorial
- It was composed of labyrinth, spongy and junctional zones with a paraplacenta
- Yolk sac haematopoiesis was still found to be present.
- The yolk sac contained endodermal acini with a specific surface glycan composition
- Trophoblast under Reichert's membrane was glycogen rich unlike that found elsewhere

1. Introduction

The West European hedgehog (*Erinaceus europaeus*) has iconic status among embryologists as it was one of the first species subjected to a detailed study of placentation [1]. Only two subsequent descriptions of the fetal membranes have been published [2,3]. Some information is available on the African hedgehogs, *Atelerix frontalis* [4,5] and *A. albiventris* [6] and the gymnure (*Echinosorex gymnura*) [7], which are also members of the Erinaceidae family.

In the present study, the placentae of a late-pregnant hedgehog were examined grossly, histologically, immunohistochemically and by lectin histochemistry to determine their structure and cellular architecture and to define the types of glycans expressed by the component maternal and fetal tissues. Such investigations are important as lectin histochemistry, applied to semi-thin sections, gives high resolution information on the cellular glycome, providing a useful tool in detecting subtle changes in the biochemistry and function of cells that are not evident using routine histological stains. Here it has been used to identify alterations in cell glycosylation that relate to the positions of cells within the placental disc and yolk sac, reflecting local differences in function and secretory ability.

2. Material and Methods

2.1. Animal

Examination of a recent road-kill hedgehog revealed a gravid uterus with 4 large pregnancy bulges, each containing a well-developed, near-term hoglet with crown-rump lengths that ranged from about 5.5 - 6.0 cm (Figure 1A). The short umbilical cords were severed to expose the flattened

22 discoid placentae. Wedges (1-2 cm wide) were cut from the outer edge towards the centre of each
23 placental disc and fixed in 10% neutral buffered formalin for 4 days.

24 *2.2. Histology and immunocytochemistry*

25 Pieces of fixed tissue were trimmed and embedded in paraffin wax for sectioning at 5µm prior to
26 staining for conventional histology with haematoxylin and eosin (H & E) or Giemsa (for the yolk
27 sac). Other sections for immunocytochemistry were dewaxed at 56˚C overnight, immersed in a
28 high pH antigen masking solution (Dako PT link; Dako UK Limited, Ely, Cambs, UK) and heated to
29 97˚C for 20 min. After cooling, the slides were rinsed in PBS and transferred to a Dako Plus
30 Autostainer (Dako UK) where a mouse monoclonal antibody generated against pancytokeratin
31 (MNF-116, Dako UK at 1:200 dilution) and appropriate secondary antibody (Dako EnVision HRP
32 labelled polymer anti rabbit and mouse antibody) were each applied for 30 mins. The secondary
33 antibody, blocking reagents, buffers, substrate, chromagen and nuclear stain were all EnVision
34 FLEX reagents (Dako UK) optimised for use in the Autostainer Plus. After staining, slides were
35 dehydrated, cleared and mounted in DPX. A negative control was run by replacing the primary
36 antibody with an unrelated monoclonal antibody.

37 *2.3. Lectin histochemistry*

38 Strips of formalin-fixed placenta were embedded in epoxy resin (TAAB Laboratories Equipment
39 Ltd., Aldermaston, UK) prior to cutting 0.75µm sections with a 3mm diamond knife and mounting
40 them on multispot slides (C.A. Hendley, Essex, UK) Ltd, composed of four wells each 12mm in
41 diameter. These were dried for 2 days at 50°C and stained with a panel of 25 lectins and an avidin-
42 biotin revealing system as previously described [8] except that SNA-1 was used at a concentration
43 of 50µg/ml. Major binding specificities of the lectins are shown in Table 1. Sections stained with

44 AHA, ECA, SBA, SNA-1, MAA, PAA and WGA were treated with 0.1 units/ml neuraminidase (0.1
45 units/ml, type VI from *Clostridium perfringens*, Sigma) for 2 h at 37°C to cleave off terminal sialic
46 acid before incubation in the lectin. Controls were carried out as previously described [8] and as a
47 control for glycogen, sections were pre-digested with 1% amylase (Sigma) in distilled water at 37°C
48 for 30 min, then washed under running water before incubation in BSA-II. Sections were examined
49 under an Olympus BX41 microscope (Tokyo, Japan) where staining intensity was assessed over 3
50 sections each of two full-depth blocks of tissue (placenta and adjoining paraplacenta) and 3
51 sections from one block of yolk sac and allocated a grade from 0 (negative) to 4 (intense staining)
52 and granule density from +/- (sparse) to ++++ (closely packed). Where there was variation in
53 staining intensity, the range is denoted in the tables.

54 **3. Results**

55 *3.1. Histology of placental disc and placental bed*

56 The placental disc comprised 3 principal zones: a labyrinth and spongy zone, both cytokeratin
57 positive (Fig. 1B, 2A) and a mixed population of cells at the fetal-maternal interface (Figs. 1F, G).
58 The fetal-facing surface (chorionic plate) contained connective tissue and small to medium size
59 branches of umbilical arteries and veins and overlay medium size maternal blood channels lined by
60 trophoblast (Fig. 1C). In all vessels, the fetal and maternal erythrocytes could be distinguished by
61 the larger size of the former (Fig 1D). Although connections between fetal capillaries could be seen
62 entering into veins, we did not encounter arteries descending through the labyrinth to supply the
63 capillaries. Occasional nucleated erythrocytes were present.

64 In the labyrinth, fetal capillaries ran parallel to trophoblast-lined maternal blood channels (Fig.
65 1D). The spongy zone, comprising trophoblast with maternal blood spaces (Fig. 1E), was less
66 extensive in this near term specimen than that described for earlier stages by Hubrecht [1] and
67 Morris [2,3]. Trophoblast cells here were often binucleate. At the fetal-maternal interface existed
68 a mixed population of cells, most of which were small with a high nuclear-to-cytoplasm ratio and
69 darkly staining nuclei, containing little or no cytokeratin. Interspersed with these were larger cells
70 that stained strongly for cytokeratin and often contained granules or vacuoles (Fig. 1F,G). They
71 occasionally formed clusters and may correspond to the trophoblast giant cells (TGCs) mentioned
72 by Carter and Enders [5], or the deciduofracts described by Hubrecht [1].

73 A thick layer of decidualised endometrium existed beneath the placental disc followed by the
74 myometrium. Many sections of maternal vessels were found in the placental bed. Sometimes they
75 were surrounded by cytokeratin-positive cells, presumed to be trophoblast, but these cells were
76 never found in the lumen, as they are in the gymnure [7], and only rarely in the tunica media.

77 Large maternal blood channels ran from the maternal side of the placental disc to the fetal surface
78 where they branched at right angles (Fig 2A); they supplied the smaller, trophoblast-lined channels
79 that ran from the fetal to the maternal side. Fetal capillaries ran parallel to them probably in the
80 opposite direction, allowing for countercurrent exchange, as suggested for the gymnure by
81 Meister and Davis [7].

82 *3.2 Lectin histochemistry of placenta*

83 The results of lectin staining are summarized in Table 1.

84 The trophoblast of the labyrinth zone contained many uniformly-sized, clear vacuoles which may
85 have been extracted fat droplets (Fig. 3A), as well as some darkly stained granules particularly
86 evident with GNA (Fig. 3B) and which also stained up with the majority of lectins (see table 1).
87 Other granules were often more threadlike and they selectively bound VVA and HPA. Surface
88 membranes strongly bound CON A, PSA (Fig. 3A), ePHA, ALA, DSA, STA, WGA and SNA-1. AHA
89 bound variably to granules, both before and after neuraminidase pre-treatment, whereas ECA and
90 SBA stained only after removal of terminal sialic acids (Figs. 3C and D). MPA, LEA and MAA bound
91 moderately-to-strongly (Figs 3E, F) but LTA less so. Only weak membrane staining was found with
92 l-PHA (Fig. 3G) and HPA and both these glycans were even more weakly expressed in the
93 cytoplasm.

94 Fetal capillaries were difficult to distinguish and the staining of their endothelial surfaces was
95 often hard to separate from erythrocyte glycan expression. The endothelial cell surface was
96 generally more glycosylated than the cytosol and bound CON A, PSA, e-PHA, MPA, (Fig. 3E), DSA,
97 STA, WGA and MAA (Fig. 3F). Both AHA and ECA stained more intensely after neuraminidase (Figs
98 3C and D); the basal surface appeared more reactive with ECA, possibly reflecting the presence of
99 basal laminae. With l-PHA (Fig. 3G), HPA, ECA and WFA, faint stippling of endothelial cell
100 cytoplasm was sometimes evident..

101 In the spongy zone, both the apical and lateral surfaces of the often-binucleate trophoblast cells,
102 (Figs 3H, I, L), were heavily glycosylated as in the labyrinth, although LEA and AHA stained less
103 prominently. The intracellular granules were more easily identifiable and these were highlighted
104 particularly well with GNA, PSA (Fig. 3H), ePHA, ALA (Fig. 3I), DSA, LEA and HPA. A certain degree
105 of intracellular heterogeneity was evident, especially with AHA (Fig. 3J). Thread-like or granular

106 inclusions that bound VVA (Fig. 3K) and HPA were again visible. These cells were rich in sialic acid,
107 reflected by a diminution in their binding of WGA after neuraminidase pre-treatment (Figs 3L, M).

108 The mixed cell population at the junction between the spongy zone and the endometrium bound
109 almost all the lectins used in the study. Amylase-sensitive glycogen, shown by BSA-II staining (Fig.
110 3N, O), was present in some of the giant cells and in the smooth muscle cells around large blood
111 vessels, though absent in both the spongy zone and labyrinth trophoblast.

112 In all areas, neuraminidase pre-treatment resulted in a loss of staining of MAA and WGA with little
113 change in SNA-1 staining. PAA remained negative while AHA, ECA and SBA staining generally
114 increased as described above. Amylase pre-treatment resulted in a loss of staining by BSA-II and
115 other controls resulted in an absence, or reduction, of staining as described previously [8].

116 *3.3. Paraplacenta*

117 Lateral to the disc (Fig. 1B) was a paraplacental structure comprising three elements (Fig. 4).
118 Innermost and facing the exocoelom was a single layer of mesothelium, continuous with a layer of
119 cells covering the placental disc. Beneath this occurred Reichert's membrane, a homogeneous
120 layer some 20-30µm thick. At the opposite side and facing the uterine epithelium were
121 cytokeratin-positive trophoblast cells (Fig. 4A). This layer of large cells, some of which were
122 binucleate or possibly multinucleate, especially near the junction with the placental disc, was 5-6
123 cells deep and it rested on a substratum of extracellular matrix interspersed with granules and
124 cells. Large nuclei could be discerned within the trophoblast cells, but there were also smaller
125 structures that were either nuclei or large vacuoles containing granules.

126 *3.4. Lectin staining of the paraplacenta*

127 The results of lectin staining are summarized in Table 2.

128 Reichert's membrane was a fibrous and heavily glycosylated structure with strong binding to
129 CONA, PSA, e-PHA, LTA, ALA, STA and SNA-1 (Fig. 4B-D). There was little or no staining with GNA,
130 l-PHA, UEA-1, BSA-1B4, DBA, VVA and BSA-II and weak to moderate binding with the remaining
131 lectins. After neuraminidase pre-treatment, staining with AHA and ECA increased while SBA and
132 WGA staining remained unchanged; PAA showed a marginal increase in binding. A distinctly
133 fibrillar substructure was seen running longitudinally through some areas of the membrane (Figs
134 4B, D and E), which probably reflected orientation of fibrils. The overlying mesothelial cells bound
135 many lectins intensely (CONA, PSA, e-PHA, ALA, MPA, WFA, DSA, STA, WGA, SNA-1, MAA, Fig 4).
136 Only UEA-1, DBA, AHA, BSA-1B_4 and -II (Fig. 4F, H, I) were unreactive and other lectins showed
137 weak staining. In some cases, suggestions of secretion by these cells could be seen on the upper
138 aspect of the membrane e.g. with WFA, DSA and AHA after neuraminidase (Figs 4E and G). Under
139 Reichert's membrane, the trophoblast cells showed heavily glycosylated cell membranes, often
140 similar to the mesothelium though with less PSA, ECA, MPA and HPA binding and more by PAA
141 after neuraminidase (Fig. 4J). Occasional membranes stained up more strongly than others (e.g.
142 with AHA, Fig 4G) and these may reflect the presence of vessels. BSA-1B_4 (Fig. 4H), LEA, SBA, WFA
143 and PAA bound strongly to the trophoblast cell membranes here while remaining negative in the
144 placental disc. Likewise, BSA-II bound to copious amounts of intracellular amylase-sensitive
145 glycogen (Fig. 4I), compared to only isolated foci in the placental junctional zone (Fig. 3N). Lectin
146 staining showed clearly the nuclear/vacuolar structures and membranous infoldings in the giant
147 cells abutting the Reichert's membrane near the placental disc (Fig. 4J).

148

149 *3.5 Histology and lectin staining of the yolk sac*

150 By late gestation, the yolk sac has been dislodged from the uterine wall, although its vasculature is
151 still supplied by the vitelline vessels (Figure 1A). Thus it is suspended in the exocoelom and lined
152 on that side by mesothelium. At the opposite surface, facing the yolk sac cavity, were columnar
153 endodermal cells (Fig 2B). In places, this layer extended down to form structures resembling acini
154 lined by endoderm (Fig. 2C), which often contained secretory material. Both these epithelia were
155 cytokeratin-positive (Fig. 5A) though less so for the inner endodermal cells, and all bore microvilli
156 that were especially prominent in the acini. The area between them contained connective tissue
157 with vitelline blood vessels and numerous haematopoietic islets (Figs 2B-F). The latter contained
158 nucleated erythrocytes at various stages of maturity (Fig. 2D), and Giemsa staining identified the
159 presence of cells with eosinophilic and small basophilic granules of indeterminate maturity (Figs.
160 2E, F).

161 The mesothelial surface of the yolk sac was heavily glycosylated (see Table 2) and it bound CON A
162 (Fig. 5B), PSA, e-PHA, ALA, MPA, GNA, DSA, STA, LEA, SNA-1, MAA, PAA and WGA. There was also
163 patchy staining with WFA, ECA and PAA and neuraminidase increased the level of staining with
164 AHA, ECA, SBA and PAA (Fig. 5C-F). There was little reduction in the heavy staining with SNA-1
165 after neuraminidase pre-treatment, or of MAA in this particular cell layer (Fig. 5G, H). There was
166 little or no staining with the other lectins. The endodermal cell surface showed a similar pattern of
167 staining apart from little binding of GNA (Fig. 5I), no staining with LEA or WFA and stronger ECA
168 staining before neuraminidase pre-treatment; PAA did not bind here at all. SBA after
169 neuraminidase (Fig. 5F) and STA showed slightly weaker staining of this layer than of the
170 mesothelium. Many diffuse endodermal granules were seen when staining with CON A, ALA, MPA,

171 and AHA and ECA after neuraminidase (Figs 5B,D); more distinct, darkly staining granules were
172 observed with PSA, e-PHA, GNA (Fig. 5I), DSA, STA, MAA, SNA-1, (Figs 5G, K) and WGA, with and
173 without neuraminidase. The inner endoderm cells and those forming the acini showed a similar
174 staining pattern to the outer cells, but often with stronger staining of the microvillous apical
175 surfaces; these also bound SBA after neuraminidase, HPA and VVA, the latter selectively (Fig. 5 J).
176 Occasional darkly staining granules (arrows) could be seen in the sub-apical cytoplasm with VVA as
177 well as intensely stained secretions in the acinar lumen, also evident with other lectins such as
178 CON A, MAA, SNA-1 and MPA (Figs 5 B, G, K and N). Inner endodermal cells, and some outer
179 ones, bound BSA-II (Fig. 5L); HPA bound in a similar pattern though more weakly (Fig. 5M). Fine
180 granules, seen in sections without obvious stain (e.g. 5C, E), were also present in the negative
181 controls. Endothelial cells were difficult to detect; they bound CON A, PSA, e-PHA, ALA, MPA (Fig.
182 5N), DSA, STA, SNA-1, MAA and WGA and also AHA and ECA after neuraminidase treatments.

183 **4. Discussion**

184 The classic paper by Hubrecht [1] gave detailed descriptions and hand-drawn illustrations of
185 almost all stages of placental development in *Erinaceus europaeus.* Morris [2, 3] extended these
186 findings by measuring nitrogen levels in the yolk sac during pregnancy, and identifying RNA,
187 glycogen, lipoidal material, reticulin, elastic tissue, mucopolysaccharides, ferric iron and alkaline
188 phosphatase in various tissues. However, his use of the Periodic-Acid-Schiff reagent gave little
189 information about the types of glycan present, which we have now resolved using lectin
190 histochemistry.

191 Both the spongy zone and the labyrinth in the placental disc of the hedgehog are composed of
192 trophoblast cells with heavily glycosylated plasma membranes. The presence of clear vacuoles in

193 these cells no doubt corresponds to the lipoidal material described by Morris [3]. Generally, the
194 pattern of lectin binding is similar in these two areas although N-acetyl glucosamine oligomers
195 (LEA) and α2,3-linked sialic acid residues (MAA) are more evident in the labyrinth. Most classes of
196 glycans are expressed, in particular complex N-linked glycans (CONA, PSA, e-PHA), α1,6-linked
197 fucosyl residues (ALA), terminal and subterminal β-galactose (AHA with and without
198 neuraminidase), subterminal N-acetyl lactosamine (ECA after neuraminidase) and N-acetyl
199 glucosamine oligomers (DSA, STA, LEA, WGA). N-acetyl galactosamine termini (VVA, HPA) are not
200 common on cell surfaces although they are present in granular or threadlike particles in the
201 spongy trophoblast which, from their profiles, may have been Golgi saccules, while subterminal
202 residues (SBA after neuraminidase) are evident in both areas. In both layers, α2,6-linked (SNA-1) is
203 more abundant than α2,3-linked (MAA) and 1,2-linked fucosyl residues (LTA, UEA-1) are generally
204 sparse. The apical surface abutting the maternal blood space shows generally greater glycosylation
205 than the lateral membranes, as would be expected to protect the fetal tissue from circulating
206 maternal antigens. A certain amount of cellular heterogeneity is evident in the distribution of
207 some glycans, especially β-galactosyl residues (AHA). Many intracellular granules are lysosomal,
208 shown by GNA binding which indicates non-reducing terminal αD-mannose residues [9] suggestive
209 of lysosomes [10]. These are most evident in the spongy trophoblast where they express most
210 glycans apart from some 1,2-linked fucosyl residues (UEA-1), terminal N-acetyl galactosamine
211 (DBA, SBA, WFA) and N-acetyl lactosamine/glucosamine oligomers bound by PAA.

212 The endothelial surface of the blood capillaries expresses all classes of glycan, the strongest being
213 complex N-glycan (CONA, PSA, e-PHA), some N-acetyl galactosamine residues (MPA), subterminal
214 β-galactose and N-acetyl lactosamine (AHA and ECA after neuraminidase) and N-acetyl
215 glucosamine and lactosamine (DSA, STA, WGA). Terminal sialic acids are strongly expressed, as in

216 most species; the high negative charges associated with sialic acid prevent the fetal erythrocytes
217 from adhering to the capillary wall.

218 The distribution of amylase-sensitive glycogen, as revealed by BSA-II staining [11], is very
219 restricted and was detected only in the mixed cell layer under the placental disc and around large
220 blood vessels in that area, confirming earlier findings by Morris [3].

221 The biochemistry and morphology of Reichert's membrane has been intensively studied in the rat
222 and mouse. It is composed mainly of filaments of type IV collagen, as in basal laminae, enclosed
223 within a laminin-containing sheath [12], in parallel layers of 3-8nm thick cords with tubular
224 structures between them. In the rat, autoradiography using ^{3}H-proline has shown that parietal
225 endodermal cells secrete proline which is incorporated into the type IV collagen of Reichert's
226 membrane [13-16]. These findings conflict with those of Duval [17] and Amoroso [18] who both
227 claimed that trophoblast secretes Reichert's membrane, as did Salamat et al. [19] who found that
228 carbohydrates are synthesised in trophoblast cells but not in parietal endoderm cells. Jollie [20],
229 however, suggested that both cell layers secrete the membrane, parts of which then fused
230 together. In the present study, the membrane was near term so it was not easy to surmise which
231 cell layer secreted the main components; MAA and WGA binding suggested that the mesothelium
232 has a more intensely stained basal plasma membrane, although it would be necessary to examine
233 membranes from earlier in gestation to be sure. Morris [2] observed that Reichert's membrane
234 increased in thickness from 5 µm in early stages to 25-30 µm at term. Our findings confirm
235 previous biochemical analyses of rat Reichert's membrane which showed galactose, mannose,
236 fucose and sialic acid to be present and higher levels of glucosamine than galactosamine [21].

237 Previous lectin studies of mouse Reichert's membrane [19] found strong binding with CON A, LTA
238 and WGA as shown here, and also with *Ricinus communis* I agglutinin which binds to terminal β-
239 galactose. AHA has a similar, but not identical, binding site which was not heavily expressed in
240 *Erinaceus*, implying a high degree of conservation in the membrane with respect to mannosyl,
241 fucosyl and N-acetyl glucosamine residues, but capping of some β-galactosyl residues in *Erinaceus.*

242 The presence of high levels of amylase-sensitive glycogen deposits in the underlying trophoblast
243 cells implies some degree of undifferentiation. In human placenta, glycogen is found in
244 cytotrophoblast cells, especially in early pregnancy [22], and is considered to be an energy source
245 for rapidly dividing cells. It is surprising, therefore, to find large amounts in near-term hedgehog
246 sub-membranous trophoblast which would no longer have to divide to any great extent to
247 accommodate the growing fetus. It was not detectable in the placental disc and the cut off of
248 glycogen deposition was quite abrupt at the junction of the membrane to the disc itself. The role
249 of the occasional giant cells found near the insertion of Reichert's membrane into the main body
250 of the placenta is not clear. The numerous membranous invaginations from the cell surface
251 suggest either fusion of several mononuclear cells or the presence of narrow channels leading to
252 the surface of the membrane, possibly for the purposes of secretion.

253 Although Morris [3] described the localisation of RNA, fats, iron, glycogen and alkaline
254 phosphatase in the yolk sac of *Erinaceus,* apart from the localisation of some PAS-positive material
255 nothing has been reported about glycan distribution. Both surfaces of the hedgehog yolk sac were
256 shown to be heavily glycosylated with both N- and O-linked glycans which reflects the metabolic
257 activity associated with yolk-sac function; both surfaces are covered with microvilli which are
258 generally associated with absorptive and enzymatic functions. The yolk sac is involved not only in

259 embryonic nutrition but also in biosynthesis and haematopoiesis [23-25] and, in other species, the
260 yolk sac synthesises a wide range of substances, including albumin, alpha-fetoprotein [26, 27] and
261 transferrin [28, 29], as well as various proteases, phosphatases and other digestive enzymes
262 [30,31]. Morris [2] reported continued entry of protein into the yolk-sac fluid during the later
263 stages of pregnancy in the hedgehog, and fibrinogen, possibly of fetal origin, was also found to be
264 present, entering the yolk-sac cavity from the vitelline vessels of the yolk-sac splanchnopleur.
265 Secretions were clearly evident in the lumina of the acini, heavily glycosylated, though their exact
266 nature was unknown.

267 The acini in the yolk sac of *Erinceus* have not previously been described, although there is a
268 structure in one of Hubrecht's figures [1] that may be a similar structure, though it is shown as a
269 solid ball of cells. The human yolk sac contains tubules which are also secretory [32] but, unlike
270 that of *Erinaceus,* the human yolk sac is a transitory structure, functioning only up to nine weeks'
271 gestation [33] after which is degenerates. The yolk sac of *Erinaceus* can also be seen to undertake
272 erythropoiesis until term, which is another unusual feature.

273 Both microvillous surfaces of the yolk sac - endodermal (inner and outer) and mesothelial -
274 expressed complex N-glycan (CON A, PSA and e-PHA) strongly, although tri/tetra-antennary non-
275 bisected glycan (l-PHA) was absent. Fucose in 1-2 linkage (UEA-1, LTA) was not detected though
276 fucose linked 1,6 was abundant throughout the yolk sac. GalNAcα1 and Galα1,3Galβ1 residues
277 bound by DBA, SBA and BSA-1B_4 were also absent, though GalNAc bound by MPA was widely
278 expressed and SBA staining increased after neuraminidase treatment, showing that some residues
279 were capped by sialic acid. GalNAcα1,6Galβ1 (WFA) was only found in patches on the
280 mesothelium. GlcNAc oligomers (DSA, STA) and N-Acetyl lactosamine (DSA, ECA) residues were

281 also found widely, some of the latter being capped with sialic acid as staining of ECA was
282 increased, especially in the mesothelium, after neuraminidase pre-treatment; GlcNAc oligomers
283 bound by LEA were restricted to the surface of the mesothelium. The presence of granules in the
284 endoderm, heavily stained with GNA, indicates non-reducing terminal a-D-mannose residues [9]
285 which are primarily markers for lysosomal glycoproteins [10] and this is probably reflects the
286 absorptive function of the endoderm. Terminal sialic acid was also present on Galβ1,3GalNAcβ1
287 bound by AHA throughout the yolk sac as staining increased after neuraminidase pre-treatment.
288 The strong staining throughout with SNA-1 was barely affected by neuraminidase pre-treatment
289 so may have had a linkage not recognized by the neuraminidase used here; α2,3-linked sialic acid
290 was also present (MAA) which was neuraminidase-sensitive apart from that on the mesothelial
291 surface. In most cases, the inner endoderm cell surfaces expressed similar sugars to the outer
292 cells, though more heavily distributed, apart from short sequences of GalNAc bound by VVA and
293 HPA which were present only on the inner endoderm cell surfaces. Occasional granules binding
294 VVA could also be seen in the inner endoderm, and could have been secretory or the result of
295 absorption; the fact that such material was not present on the surface suggests the former. The
296 endoderm cells bound amylase-sensitive BSA-II which is considered a reliable indicator of
297 intracellular glycogen [11], though its binding specificity also includes oligosaccharide chains
298 carrying terminal N-acetyl glucosamine. As previously noted [22], the same pattern of binding,
299 albeit weaker, is found with HPA, consistent with its broad specificity [34] and its ability to bind to
300 a polyglucose gel matrix [35]. The fine granules seen in many sections, including the negative
301 control, may correspond to mitochondria since similar granules of the same size were shown by
302 Morris [3] to stain positively by Kull's method for mitochondria.

303 In summary, this chance finding of a recently killed, near-term, pregnant hedgehog has enabled a
304 long- overdue, detailed description of the morphology and glycosylation of the haemochorial,
305 discoid placenta and associated tissues of the European hedgehog, *Erinaceus europaeus*.

306 **Conflict of interest**

307 The authors report no conflicts of interest. The authors alone are responsible for the content and
308 writing of the paper.

309 **Acknowledgements**

310 We are very grateful for the histological expertise of Mrs Sue Gower and also to Dr Alistair Foote
311 for performing the Giemsa staining on the yolk sac tissues.

312 **Funding**

313 This research did not receive any specific grant from funding agencies in the public, commercial, or
314 not-for-profit sectors.

315 **References**

316 [1] Hubrecht AAW. The Placentation of *Erinaceus europaeus* with remarks on the phylogeny of the
317 placenta. Quart J Microscop Sci 1889;30:283-404.

318 [2] Morris B. The yolk-sacs of *Erinaceus europaea* and *Putorius furo*. J Embryol Exp Morphol
319 1953;1:147-60.

320 [3] Morris B. Some histochemical observations on the endometrium and the yolk-sac placenta of
321 *Erinaceus europaea.* J Embryol Exp Morphol 1957;5:184-200.

322 [4] Van der Horst CJ, Gillman J. Pre-implantation phenomena in the uterus of *Elephantulus*. S Afr J
323 Med Sci 1942;7:47-71.

324 [5] Carter AM, Enders AC. Placentation in mammals once grouped as insectivores. Int J Dev Biol
325 2010;54:483-93.

326 [6] Ferner K, Siniza, S, Zeller U. The placentation of Eulipotyphla – reconstructing a morphotype of
327 the mammalian placenta. J Morphol 2014;275:1122-44.

328 [7] Meister W, Davis DD. Placentation of a primitive insectivore, *Echinosorex gymnura*. Fieldiana:
329 Zool 1953;35:11-26.

330 [8] Jones CJ, Carter AM, Aplin JD, Enders AC. Glycosylation at the fetomaternal interface in
331 hemomonochorial placentae from five widely separated species of mammal: is there evidence for
332 convergent evolution? Cells Tiss Org 2007;185:269-84.

333 [9] Shibuya N, Goldstein IJ, Van Damme EJ, Peumans WJ. Binding properties of a mannose-specific
334 lectin from the snowdrop (*Galanthus nivalis*) bulb. J Biol Chem 1988;263:728-34.

335 [10] Lityńska A, Przybylo M. Does glycosylation of lysosomal proteins show age related changes in
336 rat liver? Mech Ageing Dev 1998;102:33-43.

337 [11] Hennigar RA, Mayfield RK, Harvey JN, Ge ZH, Sens DA. Lectin detection of renal glycogen in
338 rats with short-term streptozotocin-diabetes. Diabetologia 1987;30:804-11.

339 [12] Inoué S, Leblond CP, Laurie GW. Ultrastructure of Reichert's membrane, a multilayered
340 basement membrane in the parietal wall of the rat yolk sac. J Cell Biol 1983;97:1524-37.

341 [13] Clark CC, Tomichek EA, Koszalka TR, Minor RR, Kefalides NA. The embryonic rat parietal yolk
342 sac. The role of the parietal endoderm in the biosynthesis of basement membrane collagen and
343 glycoprotein in vitro. J Biol Chem 1975;250:5259-67.

344 [14] Pierce GB, Jones A, Orfanakis NG, Nakane PK, Lustig L. Biosynthesis of basement membrane
345 by parietal yolk sac cells. Differentiation 1982;23:60-72.

346 [15] Fatemi SH. The role of secretory granules in the transport of basement membrane
347 components: radioautographic studies of rat parietal yolk sac employing ^{3}H-proline as a precursor
348 of type IV collagen. Connect Tissue Res 1987;16:1-14.

349 [16] Mazariegos MR, Leblond CP, van der Rest M. Radioautographic tracing of ^{3}H-proline in the
350 endodermal cells of the parietal yolk sac as an indicator of the biogenesis of basement membrane
351 components. Am J Anat 1987;179:79-93.

352 [17] Duval M. Le Placenta des Rongeurs. 1892, Vol 2 Felix Alcan, Paris, p. 1-640.

353 [18] Amoroso AC. Placentation. In “Marshall’s Physiology of Reproduction.” Vol.2. Ed: Parkes AS.
354 London, Longmans, 1952; p. 127-311.

355 [19] Salamat M, Götz W, Horster A, Janotte B, Herken R. Ultrastructural localization of
356 carbohydrates in Reichert's membrane of the mouse. Cell Tissue Res 1993;272:375-81.

357 [20] Jollie WP. Changes in the fine structure of the parietal yolk sac of the rat placenta with
358 increasing gestational age. Am J Anat 1968;122:513-31.

359 [21] Clark CC, Minor RR, Koszalka TR, Brent RL, Kefalides NA. The embryonic rat parietal yolk sac.
360 Changes in the morphology and composition of its basement membrane during development. Dev
361 Biol. 1975;46:243-61.

362 [22] Jones CJ, Choudhury RH, Aplin JD. Tracking nutrient transfer at the human maternofetal
363 interface from 4 weeks to term. Placenta 2015;36:372-80.

364 [23] Deren JJ, Padykula HA, Wilson TH. Development of structure and function in the mammalian
365 yolk sac. III. The development of amino-acid transport by rabbit yolk sac. Dev Biol 1966;13:370-
366 384.

367 [24] Tiedemann K, Minuth WW. Synthesis of serum proteins by the posthaematopoietic feline
368 yolk sac. Histochemistry 1980; 67:155-167

369 [25] McGrath KE, Palis J. Hematopoiesis in the yolk sac: more than meets the eye. Exp. Hematol
370 2005;33:1021-8.

371 [26] Gitlin D, Perricelli A. Synthesis of serum albumin, prealbumin, alpha-foetoprotein, alpha-1-
372 antitrypsin and transferrin by the human yolk sac. Nature 1970;228(5275):995-7.

373 [27] Nahon JL, Venetianer A, Sala-Trepat JM. Specific sets of DNase I-hypersensitive sites are
374 associated with the potential and overt expression of the rat albumin and alpha-fetoprotein genes.
375 Proc Natl Acad Sci USA 1987;84:2135-39.

376 [28] Ekblom P, Thesleff I. Control of kidney differentiation by soluble factors secreted by the
377 embryonic liver and the yolk sac. Dev Biol 1985;110:29-38.

[29] Williams CL, Priscott PK, Oliver IT, Yeoh GC. Albumin and transferrin synthesis in whole rat embryo cultures. J Exp Morphol 1986;92:33-41.

[30] Miki A, Kugler P. Comparative enzyme histochemical study on the visceral yolk sac endoderm in the rat *in vivo* and *in vitro*. Histochemistry 1984;81:409-15.

[31] Gossrau R, Graf R. Comparative hydrolase cytochemistry of the mature guinea-pig and marmoset yolk sac with special reference to proteases. Acta Histochem (Jena) 1986;80:135-47.

[32] Nogales FF, Dulcey I. The secondary human yolk sac has an immunophenotype indicative of both hepatic and intestinal differentiation. Int J Dev Biol 2012; 56:755-760.

[33] Jones CJP, Jauniaux E. Ultrastructure of the materno-fetal interface in the first trimester of pregnancy. Micron 1995; 26:145-73.

[34] Hammerström S, Murphy LA, Goldstein IJ, Etzler ME. Carbohydrate binding specificity of four N-acetyl-D-galactosamine-"specific" lectins: *Helix pomatia* A hemagglutinin, soybean agglutinin, lima bean lectin and *Dolichos biflorus* lectin. Biochemistry 1977;16:2750-5.

[35] Ishiyama I, Uhlenbruck G. On the nature of the anti-dextran activity of the *Helix pomatia* "anti A" agglutinin. Z Naturforsch B 1971;266:1198-9.

394 **List of Figures**

395 **Figure 1.** Diagram of the placenta and paraplacenta of *Erinaceus* (not to scale). Note that fetal
396 erythrocytes in the fetal capillaries are larger than the maternal red blood cells being carried in
397 the maternal channels and passing through the placenta in the maternal blood spaces which are
398 lined by trophoblast cells.

399 **Figure 2. General anatomy of the placental disc.**

400 **A.** Hoglet and placenta. Hoglet crown rump length 5.5cm. Umbilical arteries (UA) and vein (UV),
401 which show branching before reaching the placenta, can be seen as well as the vitelline vessels
402 (VV) connecting to the yolk sac (YS).

403 **B.** Overview of placental structure stained to show cytokeratin. On the right, the paraplacenta
404 with mesothelium (Mes) Reichert's membrane (RMem, unstained) and underlying cytokeratin-
405 positive trophoblast cells (Troph) can be seen. Scale bar: 200µm.

406 **C.** Chorionic plate showing a fetal artery (FA) and vein (FV) overlying a maternal blood channel
407 (MBC). H & E. Scale bar: 100 µm.

408 **D.** Labyrinth showing the arrangement of fetal capillaries (FC) running alongside maternal blood
409 spaces (MBS). Erythrocytes in fetal capillaries are larger than those in the maternal blood spaces.
410 H & E. Scale bar: 50µm.

411 **E**. Spongy zone showing maternal blood spaces (MBS); occasional binucleate trophoblast cells (*)
412 can be seen. H & E. Scale bar: 50µm.

413 **F**. Junctional zone showing cytokeratin-positive trophoblast giant cells (TGC) and smaller unstained
414 cells. Scale bar: 50µm.

415 **G.** A cluster of cytokeratin-positive trophoblast giant cells (TGC) from the junctional zone. Scale
416 bar: 25µm

417

418 **Figure 3: Placental vessel and yolk sac structure.**

419 **A**. Montage showing cytokeratin staining of a large maternal blood channel (MBC) emerging in the
420 junctional zone (JZ) and traversing the spongy zone (SZ) and labyrinth (Lab) before branching.
421 Scale bar: 200 µm.
422 **B**. Area of yolk sac showing haematopoietic islets containing nucleated erythrocytes (RBC);
423 endodermal cells face the yolk sac cavity while the mesothelium lines the exocoelom. H & E. Scale
424 bar: 50µm.
425 **C.** Part of the yolk sac containing acini lined by endoderm cells; their luminae are marked *. H & E.
426 Scale bar: 50µm
427 **D.** Haematopoietic islets of the yolk sac showing nucleated erythrocytes at various stages of
428 development as highlighted by differing nuclear sizes. A polychromatophilic normoblast can be
429 seen (arrow). Giemsa. Scale bar: 25µm
430 **E**. Cells containing eosinophilic granules (arrow) can be seen in the islets. Giemsa. Scale bar: 25µm
431 **F.** Basophilic granules are present in this islet cell (arrow). Giemsa. Scale bar: 25µm

432

433

434 **Figure 4: Lectin histochemistry of the late gestation placental disc. Scale bars: 25µm**

435 **A.** The trophoblast cells (T) of the labyrinth contain many clear vacuoles (arrows). Narrow fetal
436 capillaries (fc) run alongside maternal blood spaces (MBS) many of which are devoid of RBC in this
437 section.

438 **B.** Many granules bind GNA intensely (arrow).

439 **C**. ECA binds to fetal capillaries, especially to the basal surface. Maternal erythrocytes (Mat RBC),
440 which are smaller than those in the fetal capillaries, can be seen in the lower half of the image.

441 **D.** After neuraminidase pretreatment (+N), most cell components bind the lectin ECA.

442 **E.** MPA binds moderately to the trophoblast although fetal capillary (fc) staining is stronger.

443 **F**. MAA has a strong affinity for the fetal capillaries (fc) and less for trophoblast cytoplasm and
444 membranes.

445 **G.** Glycans binding l-PHA are poorly expressed in trophoblast but small granules that bind the
446 lectin are present in some endothelial cells (arrow).

447 **H**. In the spongy zone, binucleate trophoblast cells are clearly seen (arrows); their apical
448 (chevrons) and lateral (*) membranes in the spongy zone bind PSA strongly, as well as some
449 intracellular granules.

450 **I**. The maternal blood proteins bind ALA intensely (*) and all cell components, apart from nuclei,
451 are also bound by this lectin.

452 **J.** Heterogeneity in cell affinity for AHA by the trophoblast cells is evident.

453 **K.** Thread-like inclusions binding VVA (arrow) can be seen in the trophoblast cells.

454 **L and M.** The binding of WGA to most components of the trophoblast cells **(L)** is reduced after the
455 removal of sialic acid by neuraminidase pre-treatment (**M**).

456 **N.** BSA-II binds to components found in giant cells in the junctional zone which are amylase
457 sensitive.

458 **O**. BSA-II also binds to amylase-sensitive components in the smooth muscle cells surrounding a
459 large vessel at the base of the placental disc.

460 **Figure 5: Lectin histochemistry of the late gestation paraplacenta and associated structures.**
461 Scale bars A-G and J: 25µm, H: 100µm, I: 50µm.

462 **A.** Reichert's membrane (RM) is covered by mesothelium (Mes), neither layer appears to contain
463 cytokeratin. Underlying it are layers of trophoblast cells (T) that express the protein strongly.

464 **B**. Most components of the membrane show a strong affinity for e-PHA. A fibrillar substructure
465 within the membrane can be discerned (arrows). The matrix supporting the membrane contains
466 stained inclusions.

467 **C**. LTA stains the membrane strongly but other components only weakly.

468 **D**. SNA-1 binds to all the components of the membrane.

469 **E**. All components of the membrane bind DSA strongly and the fibrillar substructure is again
470 evident (arrow). A binucleate trophoblast cell can be seen (*) in the centre of the image.

471 **F**. With AHA, occasional vessel membranes are strongly bound.

472 **G**. After neuraminidase pre-treatment, most structures show increased staining with AHA,
473 especially the basal surface of the mesothelium, which appears to show material penetrating the
474 upper aspect of the membrane (arrow).

475 **H**. The cell membranes of the trophoblast layer under Reichert's membrane bind BSA-1B_4
476 intensely, unlike those of the spongy zone (dashed line delineates the edge of the zone) in the
477 placental disc which are completely negative. Staining ceases abruptly at the point where the
478 membrane joins the placental disc.

479 **I**. BSA-II binds to amylase-sensitive components in the trophoblast cells under the membrane.

480 **J**. Near the junction of the membrane with the main disc, occasional giant cells can be seen with
481 membranous infoldings around their abutment to the membrane (arrow). This section has been
482 stained with PAA after neuraminidase pre-treatment.

483 **Figure 6: Lectin histochemistry of the late gestation yolk sac. The same area has been captured**
484 **in all images except for A, J and N.** Scale bars 50µm except J and N which are 25 µm.

485 **A**. Yolk sac showing cytokeratin expression; outer endodermal cells (End) stain more strongly than
486 the inner cells which form acini. Nucleated RBC are in the blood islets and the mesothelium (Mes)
487 is strongly stained.

488 B. CON A binds to both surfaces and to the inner endoderm. Endodermal acini with secretions are
489 present (arrow).

490 **C.** AHA shows no binding to the yolk sac; some endodermal granules show non-specific staining.

491 **D.** After neuraminidase (+N) pre-treatment and removal of terminal sialic acid, AHA binds strongly
492 to the microvillous surfaces of both endodermal cells and mesothelium.

493 **E.** The yolk sac is virtually unstained after incubation in SBA.

494 **F.** After neuraminidase pre-treatment (+N), there is patchy staining by SBA of the surface
495 endodermal microvilli although inner cell surfaces and acini stain strongly, as does the
496 mesothelium.

497 **G.** MAA binds to α2,3-linked sialic acid which is widely expressed in all components of the yolk sac.
498 Secretions (arrow) are present in the acini.

499 **H.** Neuraminidase pre-treatment (+N) removes all MAA staining, except that of the mesothelial
500 surface.

501 **I.** Some prominent intracellular granules within the endoderm cells bind GNA strongly. These
502 probably reflect the presence of lysosomes**.**

503 **J.** Inner endodermal cell surfaces and acini (*) bind VVA strongly. Occasional sub-apical granules
504 (arrows) can be seen.

505 **K.** Almost all components of the yolk sac bind SNA-1, including secretions in the acini (*).

506 **L.** Many inner and some outer endodermal cells bind BSA-II, often showing polarisation within the
507 cells typical of glycogen deposition.

508 **M.** HPA shows a similar, although weaker, binding pattern to BSA-II.

509 **N.** Endothelial cells can be seen after staining with MPA (arrows).

Table

Click here to download Table: Hedgehog placenta table-lines 1.docx

Table 1: Lectin staining of Hedgehog placental disc and major binding specificities of the lectins.
(Staining intensity from 1 (weak) to 4 (intense). Particle density from +/- (sparse) to ++++ (abundant). Ap: apical, Lat: lateral)

Lectin	Source	Major Specificity	Placental Labyrinth Trophoblast			← Placental Spongy Zone Trophoblast →				Blood vessels	
			Surface	Cytoplasm	Granules	Ap surface	Lat surface	Cytoplasm	Granules	Surface	Cytoplasm
GNA	*Galanthus nivalis*	Glucose or mannose residues in high mannose, small, bi- tri- or tetra-antennary, bisected or non bisected complex N- linked sequences	2	2	3+++	1	1	1	3-4+++	2	1
CONA	*Canavalia ensiformis*		3	3	4++	3	2	2	4++	3	2
PSA	*Pisum sativum*		3	2	4++	3	4	2	4++	3	2
ePHA	*Phaseolus vulgaris - erythroagglutinin*		3	2-3	4+	3	3	2	4++	3	1-2
lPHA	*Phaseolus vulgaris - leucoagglutinin*		1	1	1	1	1	1	3++	1	2+
LTA	*Lotus tetragonolobus*	L-Fucose terminals linked to galactose or N-acetyl glucosamine	2	1	2+	1-2	1	1	1	1-2	1
UEA-1	*Ulex europaeus-1*		0	0	0	0	0	0	0	0	0
ALA	*Aleuria aurantia*		3	2	3+	3	3	2	4+++	2	1
MPA	*Maclura pomifera*	Galactose/αN-acetyl galactosamine	2-3	2	3+	2-3	2-3	2	3++	4	2
BSA-1B_4	*Bandeirea simplicifolia*-1B_4		0	0	0	0	0	0	0	0	0
AHA	*Arachis hypogaea*	Terminal βGalactose	3	2-3	2-3++++	1	2	1-2	3++++	1	1
AHA+N	" after neuraminidase	Subterminal βGalactose	3	3	2-3++++	3-4	3	3	3++++	3	1
ECA	*Erythrina cristagalli*	Terminal N-acetyllactosamine	0	0	0	0	0	0	0	1-3	1
ECA+N	" after neuraminidase	Subterminal N-acetyllactosamine	4	3	3-4 ++	4	3	2-3	3-4++	2-3	1
DBA	*Dolichos biflorus*	αN-acetylgalactosamine terminals	0	0	0	0	0	0	0	0	0
VVA	*Vicia villosa*		0	0	3+	0	0	0	3+++	0	0
HPA	*Helix pomatia*		1	1	3+/-	1	1	1	3-4+++	1-2	1
WFA	*Wisteria floribunda*		0	0	0	0	0	0	0	1	2+
SBA	*Glycine max*		0	0	0	0	0	0	0	0	0
SBA+N	" after neuraminidase	Subterminal αN-acetylgalactosamine	2	1-2	2-3++++	2	1-2	1-2	2-3++++	1	1
BSA-II	*Bandeirea simplicifolia*-II	Terminal α and ßNAcetyl glucosamine	0	0	0	0	0	0	0	0	0
DSA	*Datura stramonium*	N-acetyl-glucosamine oligomers and/ or N-acetyl lactosamine	4	2	3+	4	3	2	3-4++	2-3	1
STA	*Solanum tuberosum*		4	2-3	3-4+	4	3	2	3-4++	2-3	2
LEA	*Lycopersicon esculentum*		2-3	1-2	2-3+++	1	1	1	3-4+++	1	1
PAA	*Phyttolacca americana*		0	0	0	0	0	0	0	0	0
WGA	*Triticum vulgaris*	N-acetyllactosamine, di-N-acetyl chitobiose, sialic acid	3	2	3+	2-3	2-3	2	3++++	2-3	1
SNA1	*Sambucus nigra*	Terminal sialic acid	4	3	4+	4	3	3	4+	3	2
MAA	*Maackia amurensis*		2-3	1-2	3+	2	2	1-2	3+	4	2

Table

Click here to download Table: Hedgehog Table 2 -lines.docx

Table 2: Lectin histochemistry of Reichert's membrane and yolk sac.
(Staining intensity from 1 (weak) to 4 (intense). Particle density from + (sparse) to ++++ (abundant). Surf: surface, Cyt: cytoplasmic; Occ: occasional.)

Reichert's membrane

Lectin	Mesothelium		Membrane	Trophoblast		
	Surf	Cyt		Surf	Cyt	Granules
GNA	1-3	1-2	1	1	1	4+
CONA	4	2-3	3	3	1-2	4+++
PSA	4	1-2	3	1-2	1-2	4-/+
ePHA	4	1-2	3	3-4	1	4++
lPHA	1-2	1	1	1-3	1	4+
LTA	1	1	3	1	1	1
UEA-1	0	0	1	0	0	0
ALA	4	4	3	3	1-2	4++
MPA	4	1-2	2	1-3	1	3-4++
BSA-1B4	2	1	0	3	1	4+
AHA	0	0	1-2	0	0	0
AHA+N	4	1-2	2	3-4	1-2	4+
ECA	3	1	1-2	0	0	4+
ECA+N	4	1-2	2	4	1-2	2-4+++
DBA	0	0	1	0	0	0
VVA	1-2	1	0	0	0	0
HPA	1-3	1	1-2	1	1-2	3++
WFA	4	1-2	1-2	3-4	0-1	4++
SBA	1-2	0	1-2	1-3	0-1	4+
SBA+N	2	1	1-2	1-3	1	4+
BSA-II	0	0	0-1	0	1-2	4+++
DSA	4	4	2	4	1-2	4++
STA	4	3	3	4	2-3	3-4+++
LEA	3	1-2	1-2	4	2	3+
PAA	1-2	1	1	3-4	1-3	3-4+
PAA+N	2-3	1	1-2	3-4	1-3	3-4+
WGA	3-4	1	2	3-4	1-3	4++
WGA+N	3-4	1	2	3-4	1-3	4++
SNA-1	4	3	3	4	3	3-4+++
SNA-1+N	4	3	3	4	3	3-4+++
MAA	4	1-2	2	4	1-2	4+
MAA+N	1	0	1	0	0	0

Yolk Sac

Lectin	Outer endoderm			Inner endoderm			Mesothelium		Endothelium	
	Surf	Cyt	Granules	Surf	Cyt	Granules	Surf	Cyt	Surf	Cyt
GNA	1	1	Occ 4	1	1	Occ 4	3-4	3	1	1
CONA	3-4	3	3	3-4	3	3	4	2	2-1	1-2
PSA	4	1	4+	4	1	4+	4	1	3	1
ePHA	4	1	4-/+	4	1	4-/+	4	1-2	3	3
lPHA	0	0	0	0	0	0	0	0	0	0
LTA	1	1	1	1	1	1	1	1	1	1
UEA-1	0	0	2++	0	0	2+	0	0	0	0
ALA	4	2	4++	4	2	4++	4	3	4	3
MPA	3-4	2	2-3++	4	2-3	2-3++	4	2	2-3	1-2
BSA-1B4	0	0	2++	0	0	2+	0	0	0	0
AHA	0	0	2++	0	0	2+	0	0	0	0
AHA+N	4	2	2-4++	4	2-4	3-4	4	3	3-4	3
ECA	4	0	2++	3	0	2+	1-3	0	1	0
ECA+N	4	1	2-4++	4	1	2-3++	4	3	3	2
DBA	0	0	2++	0	0	2+	0	0	0	0
VVA	0	0	2^{++}	4	0	2+	0	0	0	0
HPA	1	1	2+	4	1-2	2+	1	1	0	0
WFA	0	0	2++	0	0	2+	Occ 3	0	0	0
SBA	0	0	2++	0	0	2+	0	0	0	0
SBA+N	1-3	1	2++	4	1	Occ 3	4	1	0	0
BSA-II	1-3	1-3	1-3+++	4	1	1-3+++	1-3	1	1-3	1-3
DSA	4	1	4+	4	1	4+	4	2	3	2
STA	3	1	Occ 4	3	1	Occ 4*	4	2	?3	1
LEA	0	0	2++	0	0	2+	4	1	0	0
PAA	0	0	2++	0	0	2+	3-4	0	0	0
PAA+N	1	0	2++	1-2	1	1	4	1	0	0
WGA	4	1-2	4+	4	1-2	3-4++	4	1-2	2-3	1
WGA+N	3-4	1-2	4+	4	1-2	4+	4	1-2	2	1
SNA-1	4	3	4+	4	3	4+	4	3	2-3	2-3
SNA-1+N	4	3	4+	4	3	3	4	3	2-3	2-3
MAA	3	1	4+	4	1-2	4+	4	3	3	3
MAA+N	0	0	2+	0-2	0	2+	4	1	0	0

Figure
Click here to download Figure: Hedgehod figure cartoon1.pptx

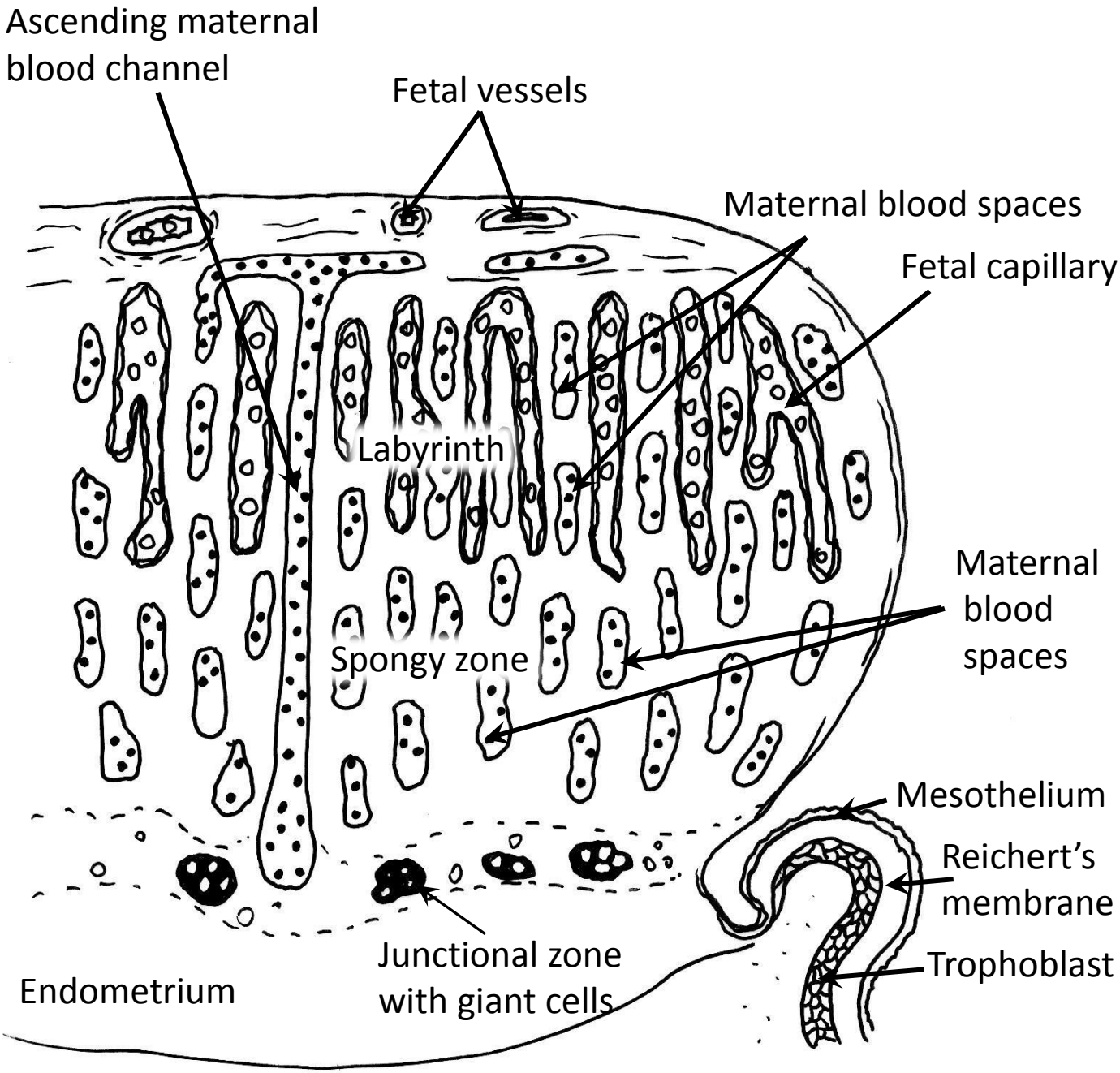

Figure

Click here to download Figure: Hedgehog Revised Figure2.pptx

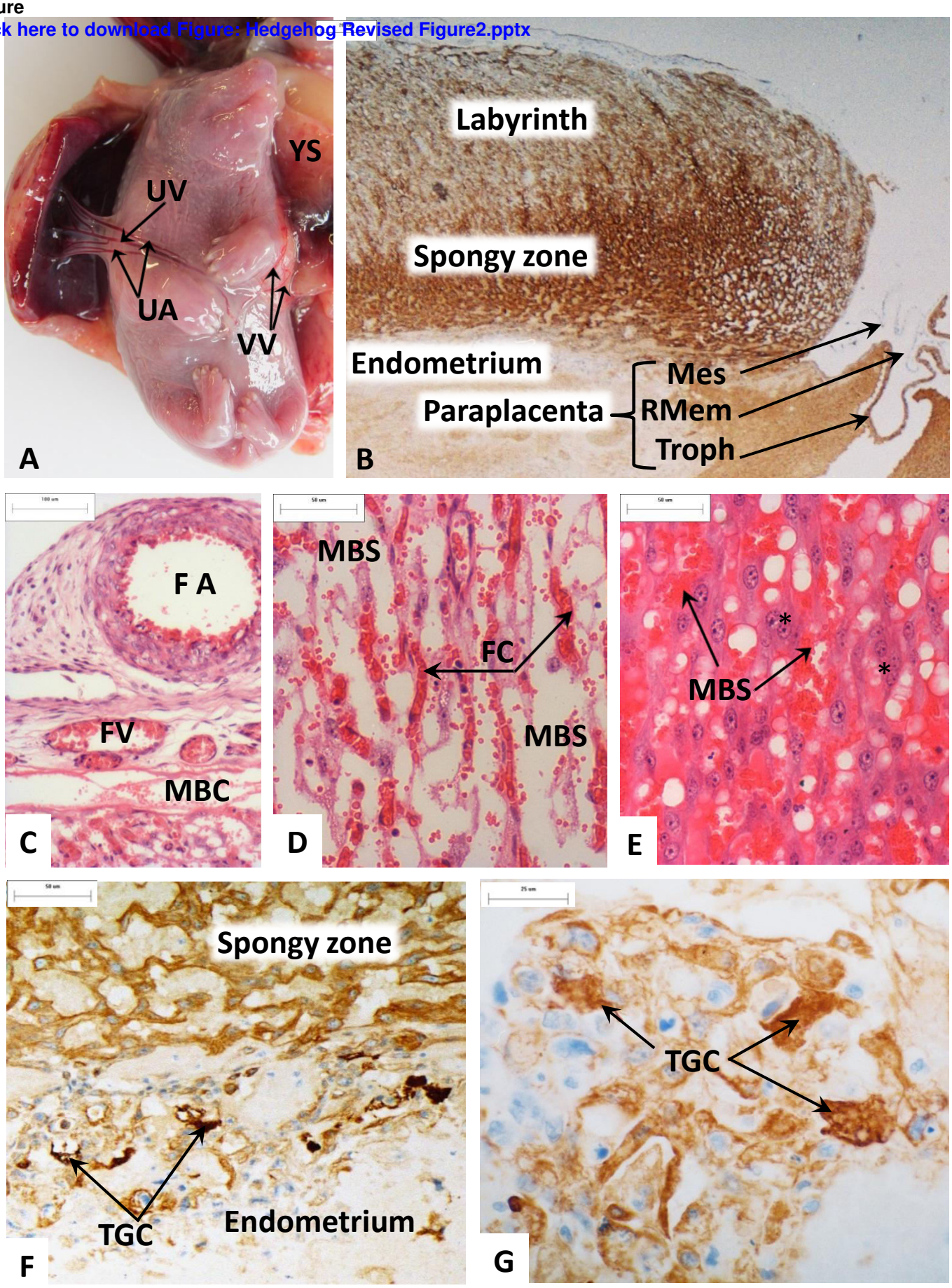

Figure

Click here to download Figure: Hedgehog Figure 3.pptx

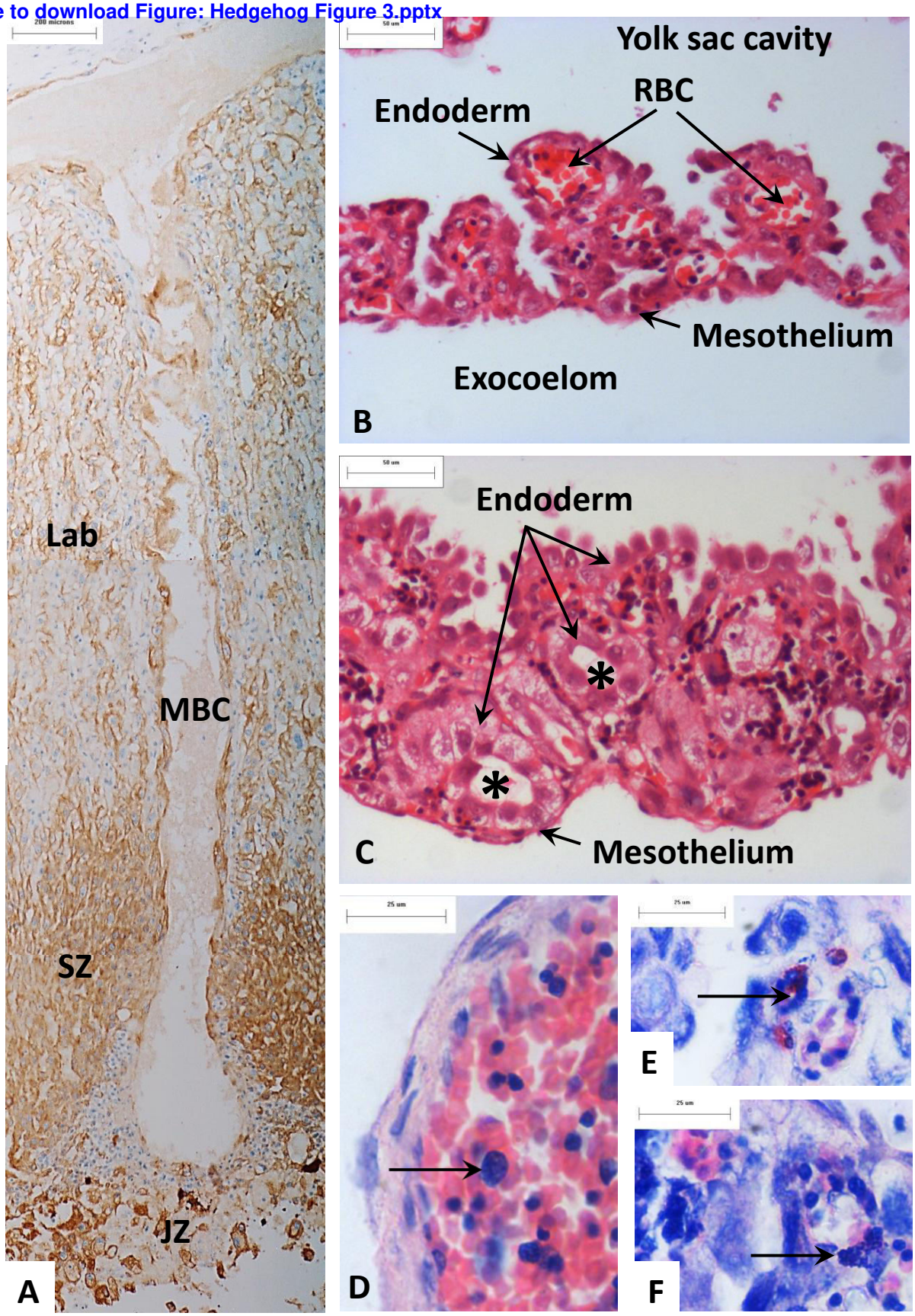

Figure

Click here to download Figure: Hedgehog Figure 4.pptx

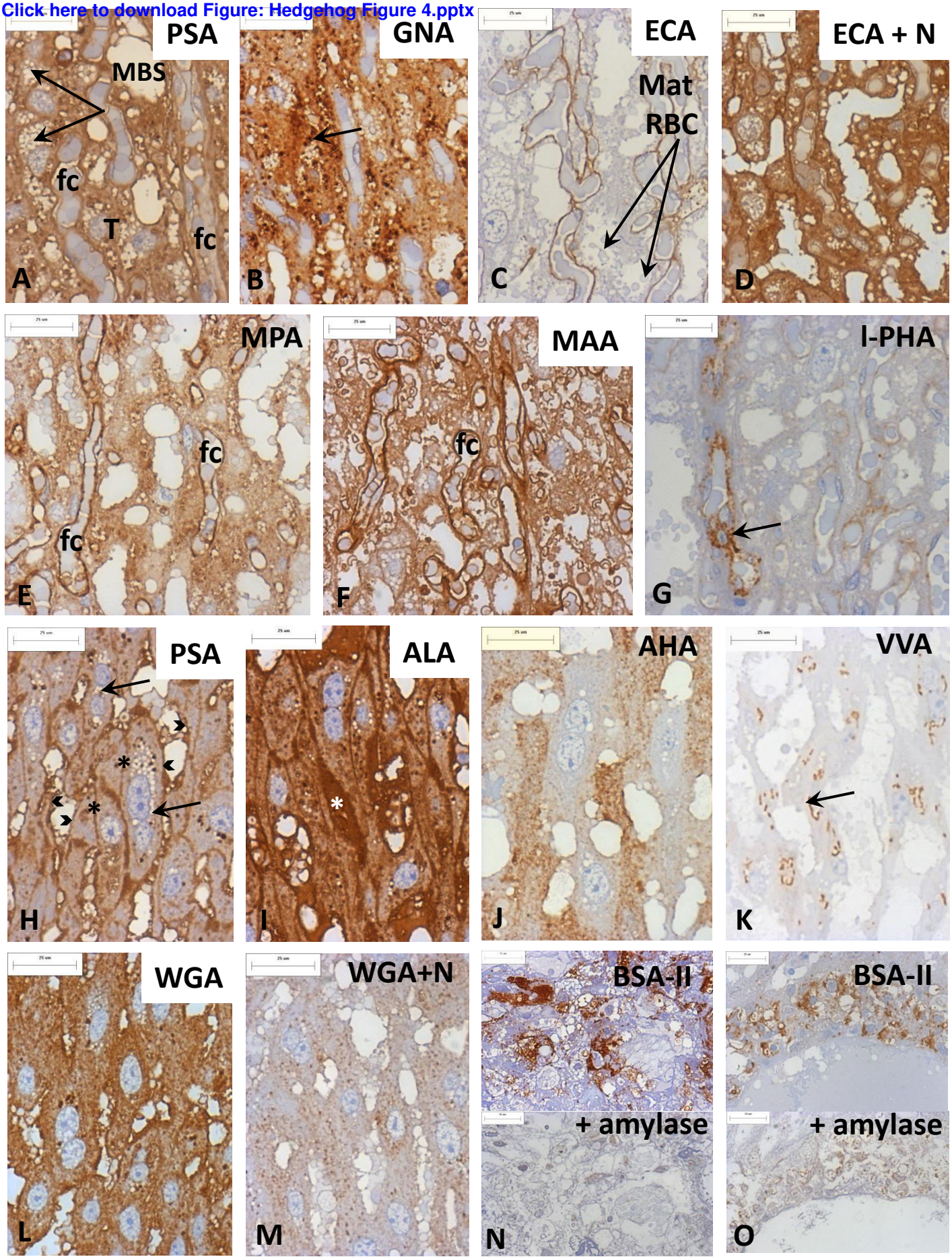

Figure
Click here to download Figure: Hedgehog Figure 5.pptx

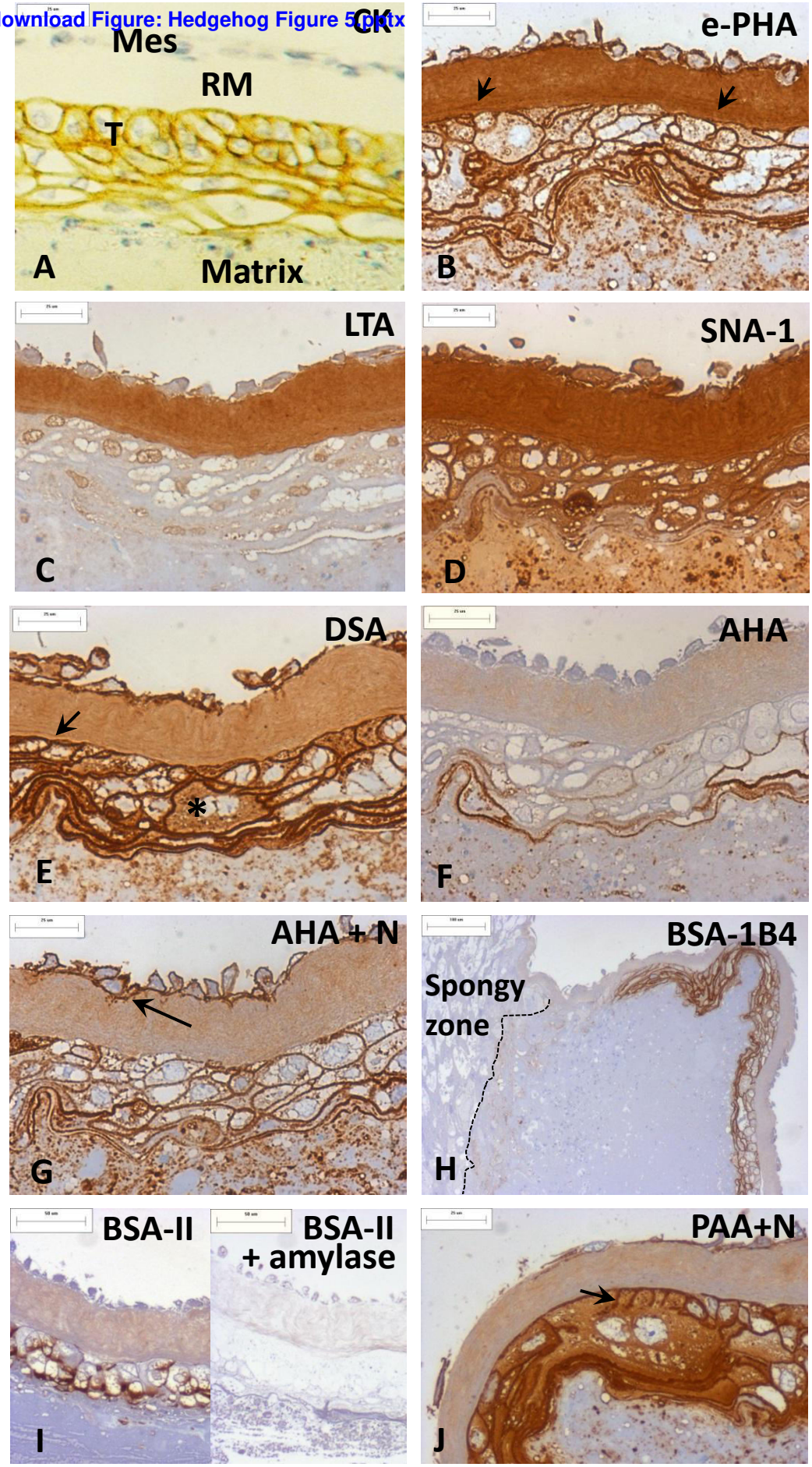

Figure

Click here to download Figure: Hedgehog Figure 6.pptx